Dyes and Pigments 90 (2011) 28–35

Contents lists available at ScienceDirect

Dyes and Pigments

journal homepage: www.elsevier.com/locate/dyepig

An experimental and theoretical study on the photophysical properties of methylene green

Carlos A. Glusko [a,b], Carlos M. Previtali [a], D. Mariano A. Vera [c,d], Carlos A. Chesta [a,*], Hernán A. Montejano [a,*]

[a] Departamento de Química, Universidad Nacional de Río Cuarto, CP 5800, Río Cuarto, Argentina
[b] Área de Cs. Básicas. Facultad de Agronomía. Universidad Nacional de La Pampa, CP 6300, Santa Rosa, La Pampa, Argentina
[c] INFIQC/CONICET, Departamento de Química Orgánica, Facultad de Química, Universidad Nacional de Córdoba. CP 3510, Córdoba, Argentina
[d] Departamento de Química, Facultad de Ciencias Exactas, Universidad Nacional de Mar del Plata, CP 7600, Mar del Plata, Argentina

ARTICLE INFO

Article history:
Received 14 April 2010
Received in revised form
5 November 2010
Accepted 8 November 2010
Available online 18 November 2010

Keywords:
Methylene green
Solvatochromic effects
Fluorescence
Triplet state
Nitro-derivatives

ABSTRACT

Methylene Green (MG) is a cationic phenothiazine dye that can be considered as a nitro derivative of methylene blue (MB). The photophysical and spectroscopical properties of MG were investigated in a wide variety of solvents, including protic and aprotic ones. The absorption ($\overline{\nu}_A$) and fluorescence ($\overline{\nu}_F$) maxima, fluorescence quantum yields and emission lifetimes were measured and correlated with the properties of the media by using the Bakhshiev's model and the empirical solvent parameter E_T^N. Fairly good linear correlations were obtained in both cases indicating the absence of specific interaction between the dye and the solvents studied. The fluorescence quantum yields were found to be in the range 0.004–0.06. Quantum mechanical calculations at the level of Density Functional Theory (DFT) and its Time-Dependent treatment for excited states (TD-DFT) performed on the ground and singlet excited states of MG (and MB) allowed finding a reasonable interpretation of the solvent effects observed on the photophysical properties of the dyes.

The triplet excited state properties of the dye were investigated by laser flash photolysis in both protic and non-protic media. In all cases, the triplet quantum yields (Φ_T) measured for MG were very small (<0.01). Triplet–triplet sensitization by duroquinone was required for the spectroscopic characterization of the triplet excited state spectrum of MG and the determination of the Φ_T in the different media. The triplet state shows important absorptions at 410, 488, and 865 nm. The molar absorption coefficient at 865 nm in acetonitrile, estimated using the depletion method, is ~30,000 M^{-1} cm^{-1}. Comparing the calculated values of the deactivation rate constants for the singlet excited states of MG and MB, it is concluded that the incorporation of the nitro group in the thiazine chromophore produces a large (~30 times) decrease of the intersystem crossing rate constant. With the aid of quantum mechanical calculations it is concluded that the intersystem crossing mechanism in both dyes differ significantly.

© 2010 Elsevier Ltd. All rights reserved.

1. Introduction

Phenothiazine photosensitisers have been used in photo-antimicrobial research for nearly 80 years (see ref. [1] for review). Methylene blue (MB) was the first synthetic dye used as an antiseptic in clinical therapy (see ref. [2] for review). In the recent years, it has been an increasing interest in these phenothiazines dyes because of their potential application in multiple disciplines such as in photodynamic therapy (PDT) [1,3–8], in the design of biosensors [9–15], as photosensitizer of ET reactions and as photoinitiators of the vinyl polymerization [16–22], etc.

Methylene Green or Basic Green 5 (MG, Scheme 1) is a cationic dye that belongs to the family of phenothiazines, which can be considered as nitro substituted derivative of MB. MG shows a considerable solubility in polar organic media and in water [23]. This dye also shows a strong absorption band ~550–690 nm, property that makes it potentially useful for PDT applications. Several reports have showed that PDT (*in vivo*) is more effective when red light is used as both the absorption and scattering of light by the tissue decrease as the wavelength increases [24,25].

Despite its potential utility of MG in PDT (and other miscellaneous applications related to cell staining and identification of biomolecules [26,27]) no systematic studies on the photophysical and spectroscopic properties of this dye have been reported. This information is decisive for understanding its photophysical/photochemical properties. In particular, the characterization of its excited

* Corresponding authors. Tel./fax.: 54 358 4676233.
E-mail addresses: cchesta@exa.unrc.edu.ar (C.A. Chesta), hmontejano@exa.unrc.edu.ar (H.A. Montejano).

0143-7208/$ – see front matter © 2010 Elsevier Ltd. All rights reserved.
doi:10.1016/j.dyepig.2010.11.003

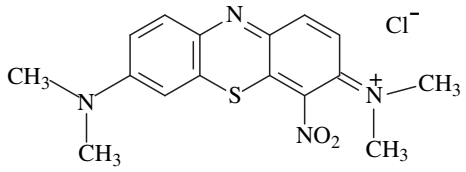

Scheme 1. Methylene Green (MG) or Basic Green 5. IUPAC Name: 7-(dimethylamino)-*N*,*N*-dimethyl-4-nitro-3H-phenothiazin-3-iminium chloride C.I. 52020.

states is of great importance to explain (and predict) its reactivity in energy transfer and/or electron transfer reactions, processes typically involved in PDT.

We report herein a detailed experimental and theoretical study of the solvent effects on the absorption, fluorescence quantum yields and emission lifetimes of MG. The properties of the triplet excited state of the dye were also investigated. The photophysical properties of MG are discussed and compared, when possible, to those of MB.

2. Materials and methods

Methylene Green chloride (MG) was purchased from Aldrich. The reported dye content of this commercial sample is ~65%. The main impurity found was methylene blue. Four other unidentified colored impurities are present in the commercial sample as could be detected by TLC. Purification was achieved by flash chromatography on silica gel (230–400 mesh) by successive elusions with methanol and water/glacial acetic acid/hydrochloric acid 50/40/10 v/v, respectively. The aqueous aliquots containing the dye were neutralized using sodium carbonate, extracted with dichloromethane, the organic phase concentrated under reduced pressure and the obtained solid dye dried under vacuum over night. The purity dye was verified by comparing the UV and fluorescence spectra with those previously reported [28,29]. Methylene Blue (MB) was purchased from Fluka (≥95%) and used as received.

All the solvents employed were HPLC grade and used as received. EtOH was distilled prior use. Water was purified using a Millipore Milli-Q system. The absence of spurious emissions of the solvents was used as purity criterion.

MG is poorly soluble in very low polarity organic media; hence, only solvents (or mixtures) with dielectric constants in the range of 6–80 were used. Fresh solutions were prepared before all measurements and the concentration of the dye was chosen to have absorbance less than 0.1 to avoid distortion of the emission spectra due to the reabsorption of the emitted light. No changes in the shape of the absorption and fluorescence spectra were observed in the 3×10^{-8}–2×10^{-5} mol/L concentration range. This can be taken as evidence of the absence of dye aggregation at concentrations $<2 \times 10^{-5}$ mol/L.

UV/Vis absorption spectra were obtained using a Shimadzu UV-2401 spectrophotometer. Steady-state fluorescence measurements were made using a Fluoromax Spex Spectrofluorometer.

Fluorescence quantum yields were determined by integration of the corrected emission spectrum using cresyl violet ($\Phi_F = 0.54 \pm 0.03$) [30] in methanol as fluorescence standard.

Fluorescence-lifetimes were measured using an Edinburgh Instruments OB 900 time-correlated single-photon counting fluorometer. The excitation was carried-out using a diode PicoQuant PLS600 with emission centered at 600 nm. In all cases the fluorescence decay times could be fitted with a monoexponential function, optimizing Chi square, residuals, and standard deviation parameters.

Transient absorption measurements were performed using a laser-flash photolysis equipment. A Spectron SL400 Nd:YAG laser generating 532 nm laser pulses (~18 ns pulse width) was used for sample excitation. The laser beam was defocused in order to cover all the path length (10 mm) of the analyzing beam from a 150 W Xe lamp. The detection system comprises a PTI monochromator coupled to a Hamamatsu R666 PM tube. The signals were initially captured by a HP54504 digitizing oscilloscope where they were averaged and then transferred to a computer for storage and analysis.

The samples were deoxygenated by continuous bubbling of high purity Ar. All measurements were performed at 25 ± 0.5 °C.

Values of relative permittivities (ε_r), refraction index (n), and empirical parameter E_T (30) of pure solvents were obtained from literature [31,32].

Density Functional Theory (DFT) Quantum calculations were done on each molecule, the ground-state geometry was optimized both in gas phase and acetonitrile at the B3LYP/6-311 + G(d,p) level of theory [33–37]. Geometry optimization was followed by harmonic vibrational frequencies calculations to verify the type of stationary point located, confirming the nature of minimum by the absence of imaginary frequencies. The solvent was modeled by means of the integral equation formalism polarized continuum model (IEFPCM) [38–40].

The excitation spectra were computed using time- dependent DFT (TD-DFT) [41] The Franck-Condon (vertical) singlet-singlet and triplet-triplet excitations energies were calculated from the optimized geometries of S_0 and T_1 states, respectively. The calculations were performed using the unrestricted formalism (UB3LYP) and the 6311 + G(d,p) basis set, suitable for open-shell systems, using the Gaussian 03 software [42]. The wavelengths in solution were obtained by the non-equilibrim solvation of the vertical excited states, since the absorption takes place much faster than the solvent reorientation [43,44]. For two relevant singlet and triplet states of MG, the relaxed structures were obtained in addition to the vertical excitations (see Table 2 and discussion). These relaxed states (S_1^*, S_0^*, T_1^* and T_2^*) were fully optimized in acetonitrile in the same way as for S_0, by assuming an equilibrium solvation (i.e., the solvent plenty repolarizes and reorganize accordingly to the self consistent excited state electronic density).

3. Results and discussion

The absorption and emission spectra of MG were studied in a series protic and non-protic media (and solvent mixtures). Fig. 1 shows the absorption and emission spectra of MG and MB in acetonitrile.

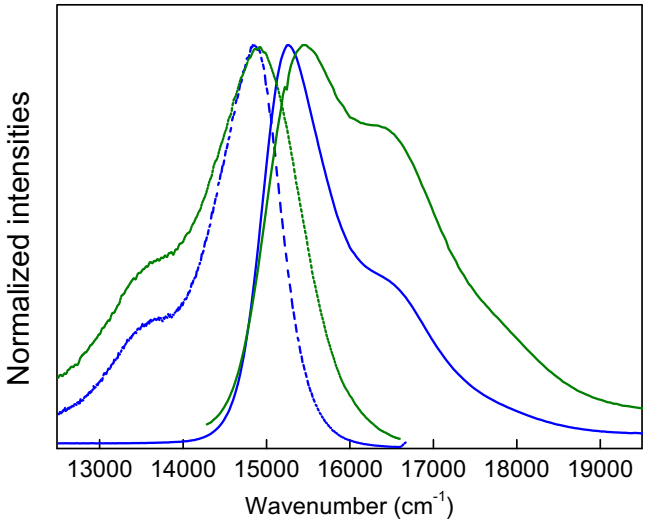

Fig. 1. Normalized absorption (solid lines) and emission (dashed lines) spectra of MG (green) and MB (blue) in acetonitrile at 298 K.

The energies of the absorption ($\bar{\nu}_A$) and fluorescence ($\bar{\nu}_F$) maxima are collected in Table 1.

Solvent effects on the Stokes' shift data ($\Delta\bar{\nu} = \bar{\nu}_A - \bar{\nu}_F$) are usually analyzed using models of varying degree of sophistication. Ultimately, these models correlate the changes observed in $\Delta\bar{\nu}$ with $\Delta\mu$ (the difference between the dipole moments of the first singlet excited and ground states) and a theoretical or empirical solvent parameter (S), i.e.:

$$\Delta\bar{\nu} = \left[(\Delta\mu)^2/a^3\right] S + C$$

where a stands for the radius of the Onsager's solvent cavity and C is a constant that depends on the nature of the chromophore. General solvent effects are commonly rationalized using Lippert [45] or Bakhshiev et al. [46] models. Bakhshiev's solvatochromic parameter (S_B) is given by equation (1):

$$S_B = \frac{2}{hc}F_1 = \frac{2}{hc}\left(\frac{\varepsilon-1}{\varepsilon+2} - \frac{n^2-1}{n^2+2}\right)\left(\frac{2n^2+1}{n^2+2}\right) \quad (1)$$

where ε and n represent the static dielectric constant and the refractive index of the medium, respectively. More recently, Ravi et al. [47] proposed an alternative model that takes into account both the specific and non-specific (general) interactions between the fluorophore and environment [48]. Ravi's solvatochromic parameter (S_R) takes the form of:

$$S_R = \frac{11307.6\ a_B^3}{\Delta\mu_B^2} E_T^N \quad (2)$$

where E_T^N is the normalized empirical microscopic solvent polarity parameter [47]. In the same equation, a_B(6.2Å) and $\Delta\mu_B$ (9.0 D) represent the solvent cavity radius and the dipole moment change measured for the reference dye *N*-phenolate betaine B [49], respectively.

It is worth to note that these models involve a large number of approximations. Among these, it is assumed that $\Delta\mu$ and a are solvent independent magnitudes. It is also supposed that the dipole moments of the vertical FC (μ_E) and the fully (geometry and solvent) relaxed (μ_E^*) singlet excited states are the same (see Fig. 3). For simplicity, the dipole moments of the relaxed (μ_G) and unrelaxed (μ_G^*) ground states are considered to be identical as well. Paradoxically, and beyond the popularity of the solvatochromic models described above, it is well known that most fluorophores do not fulfill these rough approximations [50].

Table 1
Absorption and fluorescence properties of MG in protic and aprotic solvents.

Solvent	E_T^N	F_1	$\bar{\nu}_A$ (cm^{-1})	$\bar{\nu}_F$ (cm^{-1})	τ_F[a] (ns)	Φ_F[b]
Bz/MeCN 90/10 % w/w	0.170	0.451	15319	15106	0.58	0.060
Bz/MeCN 85/15 % w/w	0.175	0.536	15321	15055	0.57	0.056
Bz/MeCN 80/20 % w/w	0.180	0.623	15314	14864	0.56	0.057
THF	0.207	0.548	15370	15027	0.78	0.060
Dichloromethane	0.309	0.596	15399	15083	0.60	0.060
2-butanone	0.327	0.767	15385	14903	0.55	0.033
1,2 dichloroethane	0.327	0.620	15342	14970	0.63	0.010
Acetone	0.355	0.790	15451	14925	0.51	0.043
Butyronitrile	0.364	0.782	15446	14948	0.59	0.063
Propionitrile	0.398	0.826	15439	15055	0.40	0.037
Acetonitrile	0.460	0.863	15466	14903	0.53	0.038
2-propanol	0.546	0.771	15352	14892	0.45	0.023
1-butanol	0.586	0.753	15509	15009	0.40	0.054
1-propanol	0.617	0.778	15392	14903	0.35	0.032
Ethanol	0.654	0.813	15439	14914	0.55	0.031
Ethanol /water 76 % v/v	0.708	0.868	15366	14717	0.38	0.020
Methanol	0.762	0.854	15516	14909	0.38	0.022
Ethanol /water 24% v/v	0.880	0.903	15342	14717	0.31	0.009
Water	1.000	0.914	15342	14892	0.33	0.004

[a] Estimated error ±2% or ±0.02 ns, whichever the greater.
[b] Estimated error ±0.005.

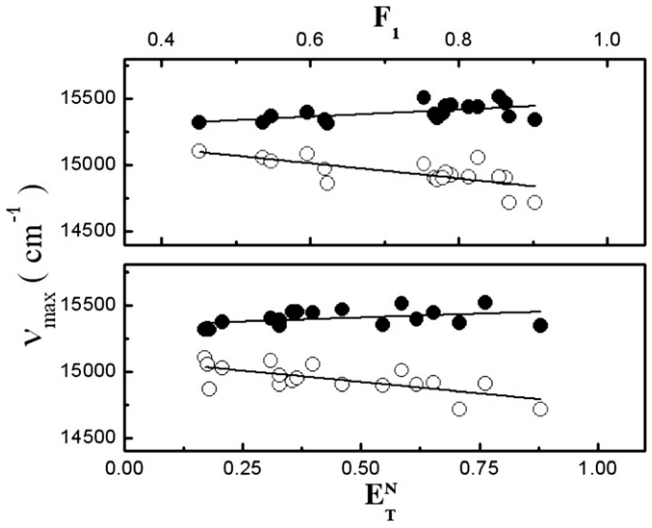

Fig. 2. Experimental $\bar{\nu}_A$ (●) and $\bar{\nu}_F$ (○) represented as a function of the solvatochromic parameters F_1 and E_T^N.

For that reason, it is often convenient to analyze the effects of the medium on the absorption and emission frequencies separately. Fig. 2 shows a plot of $\bar{\nu}_A$ and $\bar{\nu}_F$ vs. F_1 and E_T^N. As shown, fairly good linear correlations are observed in both cases. This fact suggests the lack of important specific solute-solvent interactions. Otherwise, a considerably better correlation of experimental data with empirical parameter E_T^N should have been obtained [49,51–53]. As shown in Fig. 2, $\bar{\nu}_A$ shows a slight increase with increasing F_1 (or E_T^N) while $\bar{\nu}_F$ follows the opposite trend. Within the theoretical framework of solvatochromic models considered herein the medium effects on $\bar{\nu}_A$ and $\bar{\nu}_F$ can be rationalized according to [54]:

$$\bar{\nu}_A \approx \frac{\mu_G(\mu_G - \mu_E)}{a^3} S + C_A \quad (3)$$

$$\bar{\nu}_F \approx \frac{\mu_E^*(\mu_G^* - \mu_E^*)}{a^3} S + C_F \quad (4)$$

Hence, the small positive slope of the $\bar{\nu}_A$ vs. E_T^N plot suggests that $\mu_G \geq \mu_E$, while it can be concluded that $\mu_E^* > \mu_G^*$ from the solvent dependence of $\bar{\nu}_F$. As shown bellow, these conclusions are supported by theoretical chemical calculations.

In Table 2, we present the predicted vertical singlet-singlet and singlet-triplet excitation energies (E/cm^{-1}) and the corresponding

Table 2
Theoretically predicted singlet-singlet and singlet-triplet excitation energies (E/cm^{-1}) with their corresponding oscillator strengths (f) and dipole moments (μ) calculated for some relevant states of MG and MB in the vacuum and acetonitrile.

	MG				MB			
	Vacuum		Acetonitrile		Vacuum		Acetonitrile	
	E (f)	$\|\mu\|$/D	E (f)	$\|\mu\|$/D	E (f)	$\|\mu\|$/D	E (f)	$\|\mu\|$/D
S_0	(0)	4.9	(0)	7.5	-	2.1	–	3.0
S_1	19800	6.1	17100	7.0	20000	3.3	17000	3.9
	(0.67)		(1.09)		(0.80)		(1.30)	
S_2	22000	2.7	20800	16.2	21100	6.3	20100	5.8
	(0.01)		(0.09)		(0.00)		(0.00)	
S_1^*	–	–	15600	17.3	–	–	–	–
S_0^*	–	–	8000	6.6	–	–	–	–
T_1^*	11000	4.8	10500	8.8	11000	2.9	10500	4.1
T_2^*	17050	1.8	17600	2.7	15700	6.4	15300	8.0

oscillator strengths (f) calculated from the optimized geometry of MG (and MB) in the gas phase and acetonitrile. The dipole moments (μ) of some particular states that we considered relevant for the discussion were also calculated. Details of these quantum chemical calculations are given in the experimental section.

According to the data on Table 2, both dyes should show (in acetonitrile) one allowed singlet-singlet ($S_0 \rightarrow S_1$) transition $\sim$17000 cm^{-1} and a second much less important blue-shifted ($S_0 \rightarrow S_2$) absorption around 20,800–20,100 cm^{-1}. It is worth to note that the excitation energies computed at the TD-DFT B3LYP/6-31G level of theory are estimated to be accurate within 2000–3000 cm^{-1}, usually requiring a shift towards the red to reproduce experimental spectra. [55] As shown in Fig. 1, the experimental $\bar{\nu}_A$ in acetonitrile for both dyes are at $\sim$15,400 cm^{-1} (see Fig. 1) indicating that the values of the predict excitation energies are within the expected uncertainties. Predictably, the $S_0 \rightarrow S_1$ transitions occur at higher energies in the gas phase. The calculated $\mu_G(S_0)$ and $\mu_E(S_1)$ are slightly larger in the polar solvent than in the gas phase. Although drawing definitive conclusions about the effect of the medium on μ it would be necessary to perform calculations in several media of intermediate polarity, apparently, the values of μ_G and μ_E do not change noticeably with solvent polarity. This fact may explain the nearly solvent independence observed for $\bar{\nu}_A$ (equation (3) and Fig. 2).

Interestingly, while the dipole moments calculated for S_2 states of MG in the gas phase and MB in both media are relatively small; the corresponding value for MB in acetonitrile is >16 D. An inspection of the MO involved in the $S_0 \rightarrow S_2$ transitions shows that in the first three cases that they can be considered as typical π–π^* transitions of the phenothiazine chromophore, while the latter involves a significant degree of charge transfer (CT) from the phenothiazine ring to the nitro group.

In Fig. 3 the electrostatic potentials of the solvated states corresponding to the relaxed ground (S_0), Franck-Condon (unrelaxed) singlet excited state (S_1), fully relaxed (geometry and solvent) singlet excited state (S_1^*) and the ground state (S_0^*) on the fully relaxed (geometry and solvent) singlet excited state optimized geometry (i.e., the FC emission final state), are shown.

As it can be inferred from Fig. 3, $S_1$and S_1^* differ in their geometries and dipole moments. The theoretical calculations indicate that vibrational relaxation of S_1 is accompanied by many but small changes in the internuclear distances and torsion angles, being the main change observed the pronounced rotation of the nitro group. The electrostatic potential of S_1^* clearly indicate an important degree of charge separation. Actually, this electrostatic potential reminds that of S_2 (not shown) suggesting that, at least in polarisable media, S_1relaxes to a CT state. In polar media, reorganization of the solvent's permanent dipole moments should assist charge separation during the $S_1 \rightarrow S_1^*$ relaxation process. The calculated energy of S_1^* in acetonitrile lies $\sim$15,600 cm^{-1} above S_0. The final Franck-Condon ground state (S_0^*) is $\sim$8000 cm^{-1} on top of the relaxed ground state S_0. The energy excess calculated for S_0^* is due to the fact that this state maintains both the geometry and the solvent polarization of the S_1^*. S_1^* and S_0^* differ markedly in their dipole moments; ca. $\sim$17.3 (μ_E^*) and $\sim$6.6 D (μ_G^*), respectively. Assuming that these μ do not change appreciably with solvent polarity, the difference, $(\mu_G^* - \mu_E^*) \approx -10$ D, correctly explains the negative slopes of the plots shown in Fig. 2 and consequently, the solvent dependence of $\bar{\nu}_F$ (equation (4)).

The influence of the solvent on the fluorescence lifetime (τ_F) and the fluorescence quantum yields (ϕ_F) was also investigated. The values of τ_F and ϕ_F are collected in Table 1. The ϕ_F are always small (<0.1) and the τ_F are in the subnanosecond time scale in all the media studied. The small observed fluorescence quantum yields are typical of phenothiazines dyes [56]. Both ϕ_F and τ_F have a tendency to decrease with increasing solvent polarity. From the values of $\phi_F$and τ_F, the natural florescence rate constant: $k_F \approx \phi_F/\tau_F$, and the overall non-radiative decay rate constant: $k_d + k_{isc} \approx (1-\phi_F)/\tau_F$, can be estimated. As shown in the following section, the triplet quantum yield: $\phi_T = k_{isc}\tau_F$, is always <0.01 in all the solvent inspected. This suggests that the main route for the non-radiative decay of the singlet excited state is an internal conversion process, k_d. Fig. 4 shows a plot of k_F and k_d as a function of E_T^N. The same trend is observed when these rate constants are plotted vs. F_1 indicating again the absence of important dye/solvents specific interactions. As shown in Fig. 4, k_F is almost solvent independent while k_d increases with increasing E_T^N.

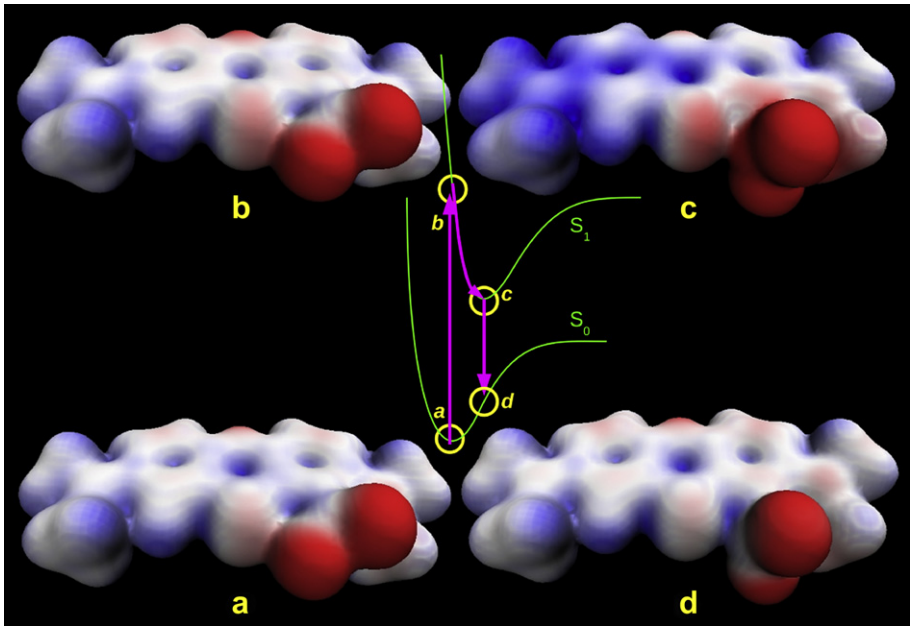

Fig. 3. Electrostatic potential corresponding to: (a) S_0, (b) the S_1, (c) S_1^* and (d) S_0^* calculated in acetonitrile. Electrostatic potential colored on an isodensity surface (0.01 a.u.) from negative (red) to positive (blue); range from 0.05 to 0.25 a.u.

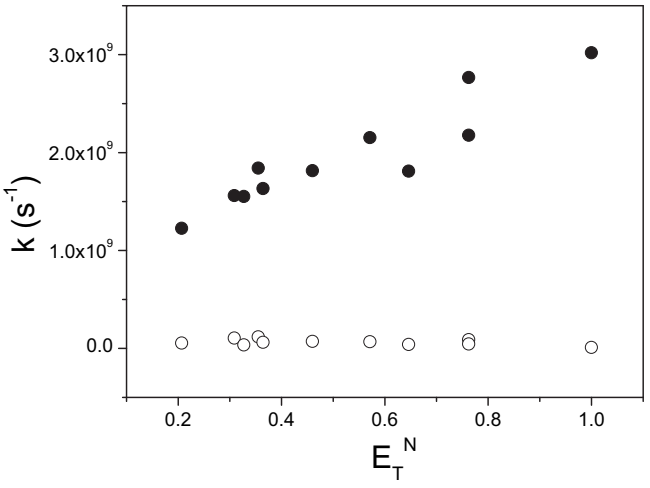

Fig. 4. Natural fluorescence rate constants (k_F, ○) and internal conversion rate constants (k_d, ●) as a function of the solvatochromic parameter E_T^N.

The observed medium effects on the non-radiative rate constant (k_d)is typical of systems involving CT states in the emission process. [57] This behavior has usually been explained using the energy gap law (golden rule). As the solvent polarity increases the energy gap between the (polar) S_1^* and S_0^* states decreases; enlarging the vibrational coupling between the two states and consequently, increasing k_d. The same principle applies to radiative rate constant k_d. However, if μ_E^* and μ_G^* do not change appreciably with solvent polarity, k_d becomes also solvent insensitive since the restrictions imposed by the golden rule can be always avoided by emission of a photon of the proper energy.

To the best of our knowledge, the triplet-triplet absorption spectrum of MG has not been reported in the literature. A possible reason for this is the apparently very low efficiency of the inter-system crossing process (step 4, Scheme 2).

Even when concentrated solutions of MG and optimized conditions of laser intensity ($\lambda_{exc} = 532$ nm) were used, the absorbance signals recorded in the 350–910 nm wavelength range were always less than 0.002. The absence of significant transient absorptions was corroborated in solvents of varied properties, such as acetonitrile, ethanol, acetone and THF. In order to characterize the triplet excited state of MG, the technique of triplet-triplet energy transfer sensitization was used. The sensitizer chosen for this purpose was the DQ ($E_T = 24{,}600$ cm^{-1} [58]). The mechanism of the triplet-triplet sensitization process is shown in the Scheme 3.

After excitation at 355 nm DQ yields quickly and efficiently its triplet excited state. [59] This process is almost completed after ~10 ns. As shown in Fig. 5, 0.3 μs (300 ns) after laser excitation the transient spectrum shows a main absorption around ~470 nm. This absorption is attributed to the ketone triplet excited state [59].

$$\mathrm{MG} \xrightarrow{h\nu_{532\,nm}} {}^1\mathrm{MG}^* \quad (1)$$

$${}^1\mathrm{MG}^* \xrightarrow{k_d} \mathrm{MG} + \mathrm{heat} \quad (2)$$

$${}^1\mathrm{MG}^* \xrightarrow{k_F} \mathrm{MG} + h\nu' \quad (3)$$

$${}^1\mathrm{MG}^* \xrightarrow{k_{isc}} {}^3\mathrm{MG}^* \quad (4)$$

$${}^3\mathrm{MG}^* \xrightarrow{k_d'} \mathrm{MG} + \mathrm{heat} \quad (5)$$

Scheme 2.

$$\mathrm{DQ} \xrightarrow{h\nu_{355\,nm}} {}^1\mathrm{DQ}^* \quad (1)$$

$${}^1\mathrm{DQ}^* \xrightarrow{k_{isc}} {}^3\mathrm{DQ}^* \quad (2)$$

$${}^3\mathrm{DQ}^* + \mathrm{MG} \xrightarrow{k_{ET}} \mathrm{DQ} + {}^3\mathrm{MG}^* \quad (3)$$

$${}^3\mathrm{MG}^* \xrightarrow{k_d'} \mathrm{MG} + \mathrm{heat} \quad (4)$$

Scheme 3.

It also apparent that the T–T energy transfer process (step 3, Scheme 3) is already taking place, as it can be concluded from the bleaching of the MG ground-state observed in the 550–680 nm wavelength range. The insert in Fig. 5 shows that the decay of the absorption at 470 nm is accompanied by the growth of a new absorption at ~865 nm. Both processes occur with similar rates, suggesting that the transient species absorbing at ~865 nm are generated by the deactivation of ^{3}DQ*. After 10 μs, the DQ triplet excited state decayed almost completely and three new absorption bands centered ~410, 490 and 865 nm become apparent. These new absorptions decay monoexponentialy with the same rate constant, rate that also agree with the slow recovery of the bleaching at ~550–680 nm. All these observations strongly suggest that the new absorptions observed in 350–500 and 700–900 wavelength ranges correspond to the triplet excited state of MG. It worth to note that a quite similar spectrum was reported for the triplet state for MB [60,61].

The triplet quantum yield (Φ_T) of MG in acetonitrile was calculated using the relative actinometry method. [62] In this method, the product $\Phi_T\varepsilon_T$ (where ε_T represents the molar absorption coefficient of the triplet state at the wavelength of analysis) is calculated by comparing the transient absorption intensities of the sample with that of an appropriate reference. In this study, the triplet-triplet absorption of zinc tetraphenyl porphyrin (ZnTPP) in benzene was used as actinometer. Values of 7.3×10^4 M^{-1} cm^{-1} and 0.83 were taken for ε_T (at 470 nm) and Φ_T for the porphyrin, respectively [63]. Strictly, the product $\Phi_T\varepsilon_T$ for the MG was calculated using equation (5):

$$(\Phi_T\varepsilon_T)_{MG} = \frac{slope_{MG}}{slope_{ZnTPP}}(\Phi_T\varepsilon_T)_{ZnTPP} \quad (5)$$

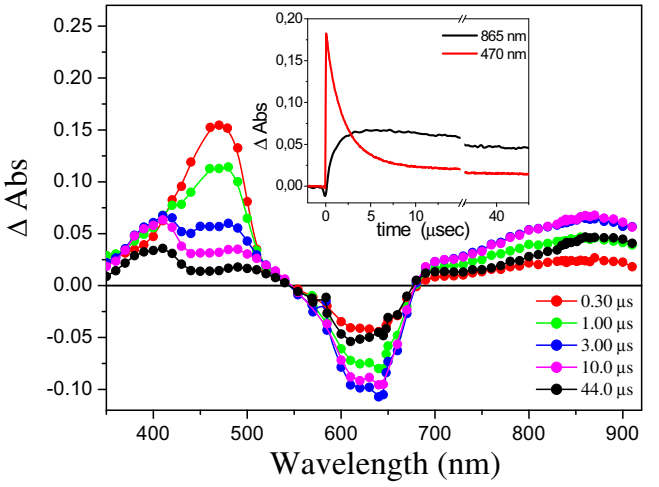

Fig. 5. Transient absorption spectra of MG 1×10^{-5} M in the presence of DQ 1×10^{-3} M in acetonitrile recorded at different times after the laser pulse. Inset: kinetic profiles at 470 nm and 865 nm. Excitation wavelength: 355 nm.

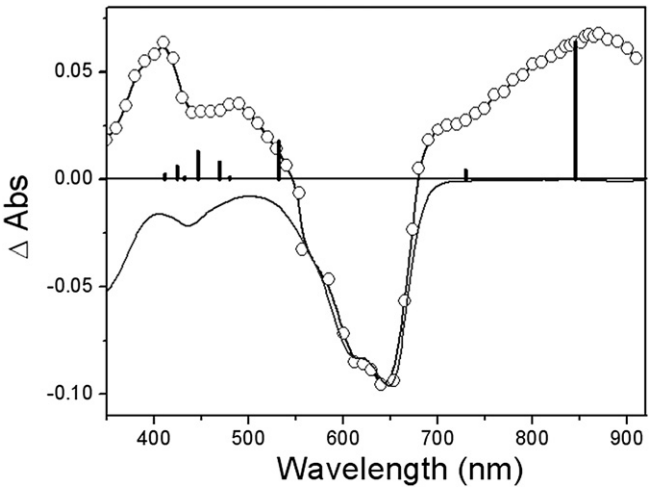

Fig. 6. Transient absorption spectrum observed at 6 μs after the laser pulse (○) and normalized ground-state absorption spectrum (—) of MG in acetonitrile. Vertical lines represent the MO calculated wavelengths for the $T_1^* \rightarrow T_n^*$ transitions and the relative values of oscillator strengths (f) normalized to the transition at 845 nm. The actual values of f are (from left to right): 0.011, 0.03, 0.004, 0.065, 0.04, 0.005, 0.09, 0.021 and 0.325 (see the text for further details).

where $slope_{MG}$ represent the initial slop of a plot of the triplet–triplet absorption of MG measured at 865 nm vs. the laser energy. Similarly, $slope_{ZnTPP}$ is the corresponding slop of the plot obtained for ZnTPP measured at 470 nm. The absorption of the dye and the reference were matched at the excitation wavelength (532 nm). Finally, in order to determine Φ_T using equation (5) the value of ε_T (at 865 nm) of the triplet-triplet absorption of the dye is required. This spectroscopic parameter was determined using the ground state depletion (GSD) method [64]. To this end, the transient negative difference absorbance at the maximum wavelength of the ground-state absorption (ΔA_G) was compared with the absorption of the triplet-triplet spectrum of the dye (ΔA_T) (both taken 6 μs after the laser pulse) according to equation (6).

$$\varepsilon_T = \left(\frac{\Delta A_T}{\Delta A_G}\right)\varepsilon_G \tag{6}$$

In equation. (6) ε_T and ε_G represent the molar absorption coefficients of the triplet and ground state at their absorption wavelength's maximum, i.e., 865 and 647 nm, respectively. The transient absorption spectrum and the normalized ground-state absorption spectrum of *MG* in acetonitrile are shown in Fig. 6. As shown, the negative absorption band caused by depletion of the ground-state closely follows the ground-state absorption band of MG, revealing the lack of formation of other photoproduct under the experimental conditions used.

Applying the procedure described above and taking into account the molar absorption coefficient (ε_G) of MG at 647 nm is 52,000 M^{-1} cm^{-1}, the values obtained for MG are $\varepsilon_T \sim 30{,}000$ M^{-1} cm^{-1} and $\Phi_T \sim (0.009 \pm 0.002)$, respectively. As it can be concluded, the triplet quantum yield is very small. This calculated Φ_T contrasts with that previously reported by Wainwright et al. [1] which was estimated (indirectly) from the quantum yield of singlet oxygen sensitization (Φ_Δ). According to these authors, the Φ_Δ value for MG is half the value reported for MB (0.52); i.e., ~0.25 [65].

Using the experimental Φ_F, τ_F and Φ_T values determined for MG in acetonitrile, all the kinetic rate constants involved in the deactivation of the singlet excited-state of the dye can be calculated. These values are $k_F = 7.0 \times 10^7$ s^{-1}, $k_{isc} = 1.7 \times 10^7$ s^{-1} and $k_d = 1.8 \times 10^9$ s^{-1}. On the other hand, taking into account that for MB $\Phi_F \sim 0.02$–0.04 (in water) [66,67] and $\Phi_T \sim 0.52$ (in ethanol) [68], the deactivation rate constants are: $k_F \sim 1.2 \times 10^8$ s^{-1}, $k_{isc} \sim 5.0 \times 10^8$ s^{-1} and $k_d \sim 4.5 \times 10^8$ s^{-1}. Hence, comparing the values of the rate constants calculated for both dyes, it can be concluded that the presence of the nitro group in the thiazine chromophore produces a large decrease (~30 times) in k_{isc} and a modest increase (~4 times) of rate constant for internal conversion, k_d.

It is well known that the incorporation of a nitro group into an aromatic chromophore generally leads to a remarkable decrease of its fluorescence quantum yield [69–71]. Diverse mechanisms have been proposed to explain the observed low emission efficiency of most substituted nitro compounds, such as: a) the enhancement of

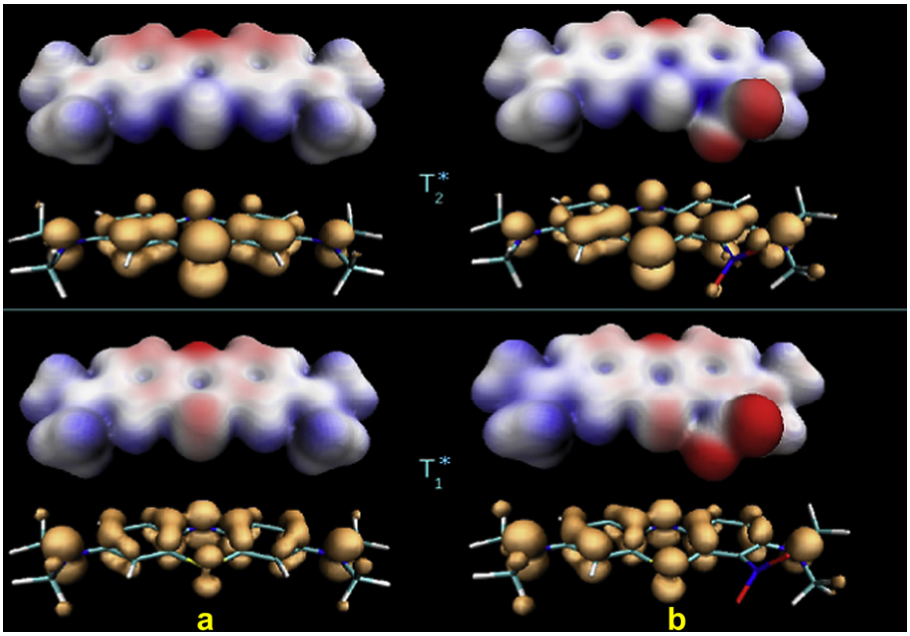

Fig. 7. Electronic properties of the T_1^* and T_2^* states of MB (a) and MG (b). Electrostatic potential colored from more negative (red, 0.05 a.u.) to more positive (blue, 0.25 a.u.) on a isosurface of electronic density (isocontour value of 0.01 a.u.). The corresponding alpha spin density isosurfaces at 0.003 a.u (golden) are shown bellow each representation of the electrostatic potentials.

the intersystem crossing quantum yield due to the presence of the NO_2 group [72–74] or b) an increase in the efficiency for internal conversion [75,76]. Unfortunately, to the best of our knowledge, no systematic experimental studies on the excited state properties of the nitro substituted compounds have been carried out, making difficult the rationalization of our results, which cannot be entirely explained by the mechanism listed above.

The electrostatic potential of the S_0, S_1 and T_1^* of MG (and MG) have similar shape. The T_1^* state corresponds to an excitation to a π^* orbital which is practically the same (despite the broken symmetry) in both dyes. This is due to the fact that this orbital is nodal in the C_{ipso} to the nitro group in MG, with no density on the NO_2 (Fig. 7). The predicted energies of the states T_1^* for both dyes are similar; ca. $\sim$10500 cm^{-1}. The energy of T_1^* for MB has been experimentally estimated (in polar solvents) to be $\sim(11500 \pm 100)$ cm^{-1} [77,78]. Hence, a reasonably good agreement between the theoretical and experimental values is observed (at least) for MB.

Furthermore, the fact that the predicted excitation $T_1^* \rightarrow T_n^*$ transition energies (Fig. 6) can reproduce acceptably well the triplet spectrum of MG is a quite encouraging result concerning the accuracy of the calculated energies. The T_2^* state is remarkably different in each dye, since the nitro group stabilizes to different extent the orbitals involved in the $T_1^* \rightarrow T_2^*$ transition (Fig. 7) shifting the energy of the T_2^*, the gap being about 2300 cm^{-1} larger in the case of MG (Table 2). In addition to this change in the energy pattern of the triplets, the role of the nitro group is also reflected in the different trend followed by the dipoles of each state (Table 2). The charge transfer character from the nitro to the phenothiazine moiety, in a sense reverse to the dipole of the T_1^* state, leads to an important decrease of the dipole of T_2^*. This fact has no parallel in the MB, where the changes in the potential from T_1^* to T_2^* have different shape and they contribute to a small increase in the polarization.

It is well establish that $S_1^* \rightarrow T_1^*$ transition can occur directly by spin-orbit coupling of S_1^* to the upper vibrational level of T_1^* or *via* spin-orbit coupling of S_1^* to an upper T_n^* state followed by fast $T_n^* \rightarrow T_1^*$ internal conversion. The S-T energy gap (golden rule) and the electronic configurations of the initial and final states are crucial in determining the intersystem-crossing mechanism. Assuming that the energy of S_1^* of MG and MB in acetonitrile are $\sim$15300 cm^{-1}, the energy gap $E_{S_1^*} - E_{T_1^*}$ is for both dyes $\sim$4000 cm^{-1}. However, while for MB the estimated energy of T_2^* is nearly isoenergetic with the experimental S_1^*, the corresponding value for MG lies above of S_1^* by more than 2200 cm^{-1}. Although this fact alone cannot fully justify the poor efficiency of the ISC process in MG; the nonexistence of a triplet state with similar energy to S_1^* provides a simple explanation based on the golden rule. Clearly, a systematic experimental and theoretical study of the properties of the excited states of nitro substituted compounds would be required to confirm this hypothesis.

4. Conclusions

The photophysical and spectroscopical properties of MG were investigated in protic and aprotic solvents. The dye shows very low fluorescence (0.004–0.06) and triplet quantum yields (<0.01) in all the solvents inspected, indicating that the singlet excited state decays mainly *via* an internal conversion pathway. The solvent effects on $\bar{\nu}_A$, $\bar{\nu}_F$, Φ_F and τ_F that specific solute-solvent interactions are not important in controlling these photophysical properties. Comparing the values of the rate constants of the deactivation of singlet excited states of MG and MB, it becomes apparent that the presence of the nitro group in the phenothiazine chromophore produces significant changes in the electronic structure of the excited states. This interpretation is supported by quantum mechanical calculations.

Acknowledgements

C.M.P., D.M.A.V., C.A.C. and H.A.M. are research staff from CONICET (Consejo Nacional de Investigaciones Cientficas y Técnicas, Argentina). C.A.G. is a Ph.D. fellow from CONICET. This work received financial support from CONICET, ANPCYT and Secretaría de Ciencia y Técnica de la Universidad Nacional de Río Cuarto, Argentina.

References

[1] Wainwright M, Mohr H, Walker WH. Phenothiazinium derivatives for pathogen inactivation in blood products. Journal of Photochemistry and Photobiology B: Biology 2007;86:45–58.
[2] Wainwright M, Crossley KB. Methylene blue – a therapeutic dye for all seasons? Journal of Chemotherapy 2002;14:431–43.
[3] Dai T, Huang YY, Hamblin MR. Photodynamic therapy for localized infections-State of the art. Photodiagnosis and Photodynamic Therapy 2009;6:170–88.
[4] Wainwright M, Phoenix DA, Marland J, Wareing DRA, Bolton FJ. A study of photobactericidal activity in the phenothiazinium series. FEMS Immunology and Medical Microbiology 1997;19:75–80.
[5] Tegos GP, Hamblin MR. Phenothiazinium antimicrobial photosensitizers are substrates of bacterial multidrug resistance pumps. Antimicrobial Agents and Chemotherapy 2006;50:196–203.
[6] Tardivo JP, Del Giglio A, Santos de Oliveira C, Santesso Gabrielli D, Couto Junqueira H, Batista Tadab D, et al. Methylene blue in photodynamic therapy: From basic mechanisms to clinical applications. Photodiagnosis and Photodynamic Therapy 2005;2:175–91.
[7] Wong TW, Wang YY, Sheu HM, Chuang YC. Bactericidal effects of toluidine blue-mediated photodynamic action on *Vibrio vulnificus*. Antimicrobial Agents and Chemotherapy 2005;49:895–902.
[8] Skripchenko A, Robinette D, Wagner SJ. Comparison of methylene blue and methylene violet for photoinactivation of intracellular and extracellular virus in red cell suspensions. Photochemistry and Photobiology 1997;65:451–5.
[9] Upadhyay AK, Ting T-W, Chen S-M. Amperometric biosensor for hydrogen peroxide based on coimmobilized horseradish peroxidase and methylene green in ormosils matrix with multiwalled carbon nanotubes. Talanta 2009;79:38–45.
[10] Barsan MM, Pinto EM, Brett CMA. Electrosynthesis and electrochemical characterisation of phenazine polymers for application in biosensors. Electrochimica Acta 2008;53:3973–82.
[11] Arechederra RL, Boehm K, Minteer SD. Mitochondrial bioelectrocatalysis for biofuel cell applications. Electrochimica Acta 2009;54:7268–73.
[12] Akers NL, Moore CM, Minteer SD. Development of alcohol/O_2 biofuel cells using salt-extracted tetrabutylammonium bromide/Nafion membranes to immobilize dehydrogenase enzymes. Electrochimica Acta 2005;50:2521–5.
[13] Li X, Zhou H, Yu P, Su L, Ohsaka T, Mao L. A Miniature glucose/O2 biofuel cell with single-walled carbon nanotubes-modified carbon fiber microelectrodes as the substrate. Electrochemistry Communications 2008;10:851–4.
[14] de Lucca AR, de S, Santos A, Pereira AC, Kubota LT. Electrochemical behavior and electrocatalytic study of the methylene green coated on modified silica gel. Journal of Colloid and Interface Science 2002;254:113–9.
[15] Svoboda V, Cooney MJ, Rippolz C, Liaw BY. In situ characterization of electrochemical polymerization of methylene green on platinum electrodes. Journal of the Electrochemical Society 2007;154:113–6.
[16] Bertolotti SG, Previtali CM. The excited states quenching of phenothiazine dyes by p-benzoquinones in polar solvents. Dyes and Pigments 1999;41:55–61.
[17] Misran M, Matthews D, Valente P, Hope A. Photochemical electron transfer between methylene blue and quinones. Australian Journal of Chemistry 1994;47:209–16.
[18] Jockusch S, Timpe H-J, Schnabel W, Turro NJ. Photoreduction of organic dyes in ketone amine systems. Journal of Photochemistry and Photobiology A: Chemistry 1996;96:129–36.
[19] Neumann MG, Rodrigues MR. The mechanism of the photoinitiation of the polymerization of MMA by the thionine-triethanolamine system. Polymer 1998;39:1657–61.
[20] Epling GA, Wang Q. Photosensitized cleavage of the dithio protecting group by visible light. Tetrahedron Letters 1992;33:5909–12.
[21] Lin C, Chang T-C. Photosensitized reduction of DDT using visible light: the intermediates and pathways of dechlorination. Chemosphere 2007;66:1003–11.
[22] Shailaja J, Sivaguru J, Robbins RJ, Ramamurthy V, Sunojb RB, Chandrasekharb J. Singlet oxygen mediated oxidation of olefins within zeolites: selectivity and complexities. Tetrahedron 2000;56:6927–43.
[23] In water MG is stable at pH <8 but decomposes in more alkaline solutions Lee C-K, Liu S-S, Juang L-C, Wang C-C, Lin K-S, Lyu M-D. Application of MCM-41 for dyes removal from wastewater. Journal of Hazardous Materials 2007;147:997–1005.
[24] Anderson RR, Parrish JA. The Optics of human skin. Journal of Investigative Dermatology 1981;77:13–9.
[25] Tegos GP, Demidova TN, Arcila-Lopez D, Lee H, Wharton T, Gali H, et al. Cationic fullerenes are effective and selective antimicrobial photosensitizers. Chemistry & Biology 2005;12:1127–35.
[26] Carter RA, Ericsson SA, Corn CD, Weyerts PR, Dart MG, Escue SG, et al. Assessing the fertility potential of equine semen samples using the reducible

dyes methylene green and resazurin. Systems Biology in Reproductive Medicine 1998;40:59–66.
[27] Li IA, Popov AM, Sanina NM, Kostetskii EY, Novikova OD, Reunov AV, et al. Physicochemical and immune properties of glycoglycerolipids from *Laminaria japonica* in immunostimulating complexes (ISCOMs). Biology Bulletin 2004; 31:244–9.
[28] Gurr E. Synthetic dyes in biology, medicine and chemistry. Academic Press; 1971.
[29] Green FJ. The Sigma–Aldrich handbook of stains, dyes and indicators. Aldrich Chemical Company Inc.; 1990.
[30] Eaton DF. Reference materials for fluorescence measurements. Pure and Applied Chemistry 1988;60:1107–14.
[31] Murov SL, Carmichael I, Hug GL. Handbook of photochemistry. 2nd ed. New York: Marcel Dekker Inc; 1993.
[32] Marcus Y. The properties of organic liquids that are relevant to their use as solvating solvents. Chemical Society Reviews 1993;22:409–16.
[33] Parr RG, Yang W. Density-funtional theory of the electronic structure of molecules. Annual Review of Physical Chemistry 1995;46:701–28.
[34] Zeigler T. Approximate density functional theory as a practical tool in molecular energetics and dynamics. Chemical Reviews 1991;91:651–67.
[35] Levine L. Quantum chemistry. 4th ed. Englewood Cliffs: Prentice-Hall; 1991. 629 pp.
[36] Becke AD. Density-funtional thermochemistry. III. The role of exact exchange. Journal of Chemical Physics 1993;98:5648–52.
[37] Lee C, Yang W, Parr RG. Development of the Colle-Salvetti correlation-energy formula into a functional of the electron density. Physical Review B 1988; 37:785–9.
[38] Cances E, Mennucci B, Tomasi J. A new integral equation formalism for the polarizable continuum model: theoretical background and applications to isotropic and anisotropic dielectrics. Journal of Chemical Physics 1997;107: 3032–41.
[39] Mennucci B, Tomasi J. Continuum solvation models: a new approach to the problem of solute's charge distribution and cavity boundaries. Journal of Chemical Physics 1997;106:5151–8.
[40] Chipman DM. Reaction field treatment of charge penetration. Journal of Chemical Physics 2000;112:5558–65.
[41] Marques MAL, Gross EKU. Time-dependent density funtional theory. Annual Review of Physical Chemistry 2004;55:427–55.
[42] Frisch MJ, et al. Gaussian 03, Rev. B.04. Wallingford, CT: Gaussian, Inc., http://www.gaussian.com; 2003.
[43] Cossi M, Barone V. Time-dependent density functional theory for molecules in liquid solutions. Journal of Chemical Physics 2001;115:4708.
[44] Impronta R, Barone V, Scalmani G, Frisch MJ. A state-specific polarizable continuum model time dependent density functional method for excited state calculations in solution. Journal of Chemical Physics 2006;125:054103.
[45] Lippert Von E. Spektroskopische bistimmung des dipolmomentes aromatischer verbindungen im resten angenegten singulettzustand. Z. Electrochem 1957;61:962–75.
[46] Bakhshiev NG, Knyazhanskii MI, Minkin VI, Osipov OA, Saidov GV. Experimental determination of the dipole moments of organic molecules in excited electronic states. Russian Chemical Reviews 1969;38:740–54.
[47] Ravi M, Samanta A, Radhakrishnan TP. Excited state dipole moments from an efficient analysis of solvatochromic stokes shift data. Journal of Physical Chemistry 1994;98:9133–6.
[48] Reichardt C. Solvatochromic dyes as solvent polarity indicators. Chemical Reviews 1994;94:2319–58.
[49] Cunderlikova B, Sikurova L. Solvent effects on photophysical properties of merocyanine 540. Chemical Physics 2001;263:415–22.
[50] Painelli A, Terenziani F. A non-pertuvative approach to solvatochromic shifs of push-pull chromophores. Chemical Physics Letters 1999;312:211–20.
[51] Lakowicz JR. Principles of fluorescence spectroscopy. Chapter 5. 2nd ed. Ney York: Kluwer Academic/Plenun Publishers; 1999.
[52] Gómez ML, Previtali CM, Montejano HA. Photophysical properties of safranine O in protic solvents. Spectrochimica Acta Part A 2004;60:2433–9.
[53] Broglia MF, Bertolotti SG, Previtali CM, Montejano HA. Solvatochromic effects on the fluorescence and triplet–triplet absorption of phenosafranine in protic and aprotic solvents. Journal of Photochemistry and Photobiology A: Chemistry 2006;180:143–9.
[54] Amos AT, Burrows BL. Advances in Quantum Chemistry 1973;7:298–312.
[55] Kowalczyk M, Sikorska E, Khemelinskii IV, Komasa J, Insinska-Rak M, Sikirski M. Spectroscopy and photophysics of flavin-related compounds: isoalloxazines. Journal of Molecular Structure, THEOCHEM 2005;756:47–54.
[56] Elisei F, Latterini L, Aloisi G, Mazzucato U, Viola G, Miolo G, et al. Excited-state properties and in vitro phototoxicity studies of three phenothiazine derivatives. Photochemistry and Photobiology 2002;75:11–21.
[57] Biczók L, Bérces T, Márta Ferenc, Substituen Solvent, Temperature Effects. on Radiative and Nonradiative Processes of Singlet Excited Fluorenone Derivatives. Journal of Physical Chemistry 1993;97:8895–9. and references therein.
[58] Scheerer R, Grätzel M. Laser photolysis studies of duroquinone triplet state electron transfer reactions. Journal of the American Chemical Society 1977; 99:865–71.
[59] (a) Amouyal E, Bensasson R. Interaction of duroquinone lowest triplet with amines. Journal of the Chemical Society, Faraday Transactions 1: Physical Chemistry in Condensed Phases 1977;73:1561–8;
(b) Bisby RH, Parker AW. Reactions of excited triplet duroquinone with a-tocopherol and ascorbate: a nanosecond laser flash photolysis and time-resolved resonance raman investigation. Journal of American Chemical Society 1995;117:5664–70;
(c) Zhu G, Wu G, Sha M, Long D, Yao S. Effects of ionic liquid [bmim][PF6] on absorption spectra and reaction kinetics of the duroquinone triplet state in acetonitrile. Journal of Physical Chemistry A 2008;112:3079–85.
[60] Ohno T, Osif TL, Lichtin NN. A previously unreported intense absorption band and pK of protonated triplet methylene blue. Photochemistry and Photobiology 1979;30:541–6.
[61] Kamat PV, Lichtin NN. Electron transfer in the quenching of protonated triplet methylene blue by ground-state molecules of the dye. Journal of Physical Chemistry 1981;85:3864–8.
[62] Carmichael I, Hug GL. Triplet–triplet absorption spectra of organic molecules in condensed phases. Journal of Physical and Chemical Reference Data 1986;15:1.
[63] Hurley JK, Sinai N, Linschitz H. Actinometry in monochromatic flash photolysis: The extinction coefficient of triplet benzophenone and quantum yield of triplet zinc tetraphenyl porphyrin. Photochemistry and Photobiology 1983; 38:9–14.
[64] Bonneau R, Carmichael I, Hug GL. Molar absorption coefficients of transient species in solution. Pure and Applied Chemistry 1991;63:289–99.
[65] Fernandez JM, Bilgin MD, Grossweiner LI. Singlet oxygen generation by photodynamic agents. Journal of Photochemistry and Photobiology B: Biology 1997;37:131–40.
[66] Olmsted J. Calorimetric determinations of absolute fluorescence quantum yields. The Journal of Physical Chemistry 1979;83:2581–4.
[67] Varga O, Kubinyi M, Vidóczy T, Baranyai P, Bitter I, Kállay M. Methylene blue–calixarenesulfonate supramolecular complexes and aggregates in aqueous solutions. Journal of Photochemistry and Photobiology A: Chemistry 2009;207:167–72.
[68] Nemoto M, Kokubun H, Koizumi M. Determination of the S^*–T transition probabilities of some xanthene and thiazine dyes on the basis of the T-Energy transfer. I. Experiment in ethanol solutions. Bulletin of the Chemical Society of Japan 1969;42:1223–30.
[69] Görner H, Fischer C, Daub J. Photoreaction of dihydroazulenes into vinylheptafulvenes: photochromism of nitrophenyl-substituted derivatives. Journal of Photochemistry and Photobiology A: Chemistry 1995;85:217–24.
[70] Rtishchev N, Samoilov D, Martynova V, El′tsov AV. Luminescence properties of nitro derivatives of fluorescein. Russian Journal of General Chemistry 2001; 71:1467–78.
[71] Beinhoff M, Weigel W, Jurczok M, Rettg W, Modrakowski C, Brudgam I, et al. Synthesis and spectroscopic properties of arene-substituted pyrene derivatives as model compounds for fluorescent polarity probes. European Journal of Organic Chemistry 2001;2001:3819–29.
[72] Chow YL. In: Patei S, editor. The chemistry of amino, nitroso and nitro compounds and their derivatives. N.Y: John Wiley & Sons; 1982. p. 181. Suppl. F.
[73] Guglielmetti R. In: Dürr H, Bouas-Laurent H, editors. Photochromism-molecules and systems, studies in organic chemistry, vol. 40. Amsterdam: Elsevier; 1990. p. 314.
[74] Görner H, Fischer C. Reversible photochemistry of 4-nitro-substituted diphenylazomethines. Journal of Photochemistry and Photobiology A: Chemistry 1991;57:235–46. and references therein.
[75] Samori S, Tojo S, Fujitsuka M, Spitler EL, Haley MM, Majima T. Donor–acceptor-substituted tetrakis(phenylethynyl)benzenes as emissive molecules during pulse radiolysis in benzene. Journal of Organic Chemistry 2007;72:2785–93.
[76] Gunaratne T, Reddy Challa J, Cather Simpson M. Energy flow in push–pull chromophores: vibrational dynamics in *para*-nitroaniline. ChemPhysChem 2005;6:1157–63.
[77] Kearns DR, Hollins RA, Khan AU, Chambers RW, Radlick P. Evidence for the participation of $^1\Sigma g+$ and $^1\Delta g$ oxygen in dye-sensitized photooxygenation reactions. Journal of the American Chemical Society 1967;89:5455–6.
[78] Ohno T, Lichtin NN. Electron transfer in the quenching of triplet methylene blue by complexes of iron (II). Journal of the American Chemical Society 1980;102:4636–43.